

Boundary quantum critical phenomena with entanglement renormalization

G. Evenbly,¹ R. N. C. Pfeifer,¹ V. Picó,² S. Iblisdir,² L. Tagliacozzo,¹ I. P. McCulloch,¹ and G. Vidal¹

¹*School of Physical Sciences, The University of Queensland, Queensland 4072, Australia*

²*Depto. Estructura i Constituents de la Materia, Universitat Barcelona, 08028 Barcelona, Spain*

(Received 11 October 2010; published 29 October 2010)

We propose the use of entanglement renormalization techniques to study boundary critical phenomena on a lattice system. The multiscale entanglement renormalization ansatz (MERA), in its scale invariant version, offers a very compact approximation to quantum critical ground states. Here we show that, by adding a boundary to the MERA, an accurate approximation to the ground state of a semi-infinite critical chain with an open boundary is obtained, from which one can extract boundary scaling operators and their scaling dimensions. As in Wilson's renormalization-group formulation of the Kondo problem, our construction produces, as a side result, an effective chain displaying explicit separation of energy scales. We present benchmark results for the quantum Ising and quantum XX models with free and fixed boundary conditions.

DOI: [10.1103/PhysRevB.82.161107](https://doi.org/10.1103/PhysRevB.82.161107)

PACS number(s): 64.70.Tg, 03.67.-a, 05.50.+q, 11.25.Hf

Recent progress in the understanding of many-body entanglement has led to novel ways to represent the ground state of lattice systems. In particular, scale invariant ground states, corresponding to the fixed points of the renormalization group (RG) flow, can be accurately approximated with the multiscale entanglement renormalization ansatz (MERA).^{1,2} This variational ansatz consists of a set of tensors, known as *disentangler*s and *isometries*, that are connected according to a characteristic, self-similar pattern of layers, see Fig. 1, where each layer corresponds to a different length scale. Remarkably, the same simple tensor network (conveniently adapted to the spatial dimensions and geometry of the lattice) can describe a large variety of ground states by just varying the parameters encoded in the disentanglers and isometries. Indeed, the scale invariant MERA has been used to describe noncritical RG fixed points of symmetry-breaking phases and topologically ordered phases,³ as well as critical RG fixed points, corresponding to continuous quantum phase transitions.^{1,2,4-7}

In this Rapid Communication, we introduce entanglement renormalization techniques for the study of boundary critical phenomena. We propose a MERA *with a boundary* as an ansatz for the scale invariant ground state of a semi-infinite one-dimensional lattice at a quantum critical point. In addition to the bulk disentangler u and bulk isometry w used to describe the system in the absence of a boundary, this ansatz is also characterized by a boundary isometry w^\diamond , see Fig. 2, from which the boundary scaling dimensions of the system can be extracted. The boundary MERA offers a significant advantage over other numerical methods, such as Wilson's numerical RG (NRG) (Ref. 8) and White's density-matrix renormalization group,⁹ which are based on a matrix product state (MPS).¹⁰ Recall that the presence of an open boundary, which is felt everywhere in the bulk with a strength that only decays as a power law of the distance to that boundary, explicitly breaks translation invariance. As a result, a proper characterization of boundary critical phenomena requires simulating large systems with a computational cost that, with an inhomogeneous MPS, is at least proportional to the system size. By exploiting scale invariance, the boundary MERA can instead address the thermodynamic limit directly, encoding the ground state in just three tensors (u, w, w^\diamond).

Bulk MERA. Recall that the scale invariant MERA for an infinite critical chain without a boundary^{1,2,4-7} is characterized by a unique pair of bulk tensors, namely, a disentangler u and an isometry w , distributed in layers according to Fig. 1(i). A layer of disentanglers and isometries defines a real-space RG transformation that can be used to coarse grain the original lattice \mathcal{L} , producing a sequence of effective lattices $\{\mathcal{L}, \mathcal{L}', \mathcal{L}'', \dots\}$. Under coarse graining, a local operator o transforms according to the scaling superoperator \mathcal{S} , Fig. 1(ii),

$$o \xrightarrow{\mathcal{S}} o' \xrightarrow{\mathcal{S}} o'' \dots \quad (1)$$

A *scaling operator* ϕ_α is a special type of operator that, under coarse graining, transforms into itself times some scaling factor. The scaling operators ϕ_α and scaling dimensions Δ_α are obtained from the eigenvalue decomposition of the scaling superoperator \mathcal{S} ,^{5,6}

$$\mathcal{S}(\phi_\alpha) = \lambda_\alpha \phi_\alpha, \quad \Delta_\alpha \equiv -\log_3 \lambda_\alpha, \quad (2)$$

where the base 3 of the logarithm reflects the fact that the coarse-graining transformation maps three sites into one. Recall that from the scaling dimensions, which govern the decay of two-point correlators in the bulk, Fig. 1(iii),

$$\langle \phi_\alpha(r) \phi_\alpha(r') \rangle = \frac{1}{|r - r'|^{2\Delta_\alpha}}, \quad (3)$$

one can extract the critical exponents of the model. In fact, most of the data that characterizes the conformal-field theory (CFT) (Ref. 11) associated to a critical chain can be extracted from the scale invariant MERA.⁶

Boundary MERA. In order to represent the ground state of a semi-infinite, quantum critical spin chain, we propose to use the ansatz described in Fig. 2(i), which is obtained by adding a boundary, made of copies of a boundary isometry w^\diamond , to a section of the scale invariant MERA used for the bulk. Importantly, the tensors (u, w) are *the same* that are used to describe the bulk in the absence of a boundary. As a result, the boundary MERA defines a real-space RG transformation that, off the boundary, is identical to that of the bulk

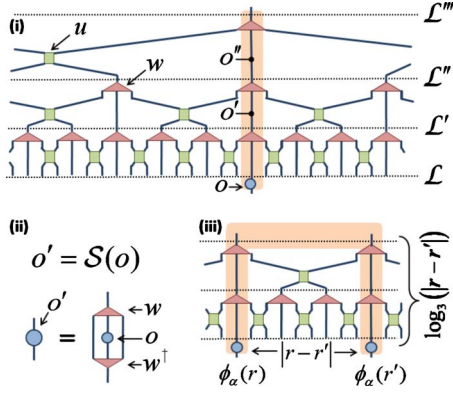


FIG. 1. (Color online) (i) Scale invariant MERA, as characterized by a bulk disentangler u and bulk isometry w . (ii) Scaling superoperator \mathcal{S} for one-site local operators o , in terms of the bulk isometry w . (iii) Computation of a two-point correlator $\langle \phi_\alpha(r) \phi_\alpha(r') \rangle$ for a scaling operator ϕ_α and selected sites r and r' , Eq. (3). After $\log_3(|r-r'|)$ coarse-graining transformations, the two copies of ϕ_α become nearest neighbors and fuse into the identity with unit amplitude (by normalization of ϕ_α). Each coarse-graining step multiplies ϕ_α by $3^{-\Delta_\alpha}$, resulting in a power-law decay (see Ref. 6 for details).

MERA, Eq. (1). However, a local operator o^\diamond at the boundary transforms according to the *boundary scaling superoperator* \mathcal{S}^\diamond , that depends only on the isometry w^\diamond , Fig. 2(ii),

$$o^\diamond \xrightarrow{\mathcal{S}^\diamond} o^{\diamond'} \xrightarrow{\mathcal{S}^\diamond} o^{\diamond''} \dots \quad (4)$$

This allows us to identify a new set of scaling operators, namely, the *boundary scaling operators* ϕ_α^\diamond and corresponding scaling dimensions Δ_α^\diamond , which are obtained from the eigenvalue decomposition of \mathcal{S}^\diamond ,

$$\mathcal{S}^\diamond(\phi_\alpha^\diamond) = \lambda_\alpha^\diamond \phi_\alpha^\diamond, \quad \Delta_\alpha^\diamond \equiv -\log_3 \lambda_\alpha^\diamond. \quad (5)$$

As argued in Fig. 2(iii), a correlator between a boundary scaling operator ϕ_α^\diamond and a bulk scaling operator ϕ_β reads

$$\langle \phi_\alpha^\diamond(0) \phi_\beta(r) \rangle \approx \frac{C_{\alpha\beta}}{r^{\Delta_\alpha^\diamond + \Delta_\beta}}. \quad (6)$$

Recall that in a critical system without a boundary the expectation value of any scaling operator (other than the identity $\mathbb{1}$) vanishes, $\langle \phi_\beta(r) \rangle_{\text{bulk}} = 0$, whereas in the presence of a boundary the same expectation value decays as a power law with the distance to the boundary, as described by a boundary CFT (BCFT).^{11,12} This characteristic feature of boundary critical phenomena is readily reproduced by taking ϕ_α^\diamond to be the identity operator $\mathbb{1}^\diamond$ (with vanishing scaling dimension) in Eq. (6),

$$\langle \phi_\beta(r) \rangle \approx \frac{C_{0\beta}}{r^{\Delta_\beta}}. \quad (7)$$

Effective lattice. Additional insight into the boundary MERA is obtained by using the bulk disentanglers and isometries to transform the original critical lattice \mathcal{L} into an ef-

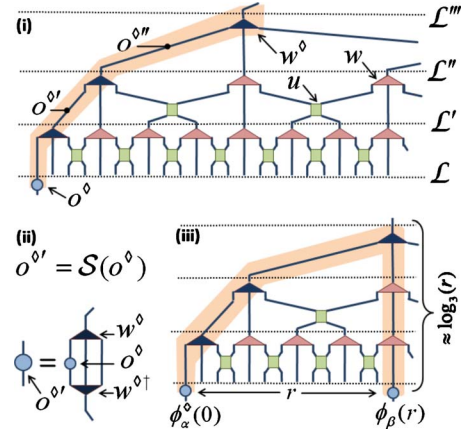


FIG. 2. (Color online) (i) Scale invariant MERA with a boundary, as characterized by the bulk tensors u and w of Fig. 1 and a boundary isometry w^\diamond . (ii) Scaling superoperator \mathcal{S}^\diamond for boundary operators o^\diamond , in terms of the boundary isometry w^\diamond . (iii) Computation of a two-point correlator $\langle \phi_\alpha^\diamond(0) \phi_\beta(r) \rangle$ for a boundary scaling operator ϕ_α^\diamond and a bulk scaling operator ϕ_β , Eq. (6), with $r = (3^{t+1} - 1)/2$. After $t \approx \log_3(r)$ coarse-graining transformations, ϕ_α^\diamond and ϕ_β become nearest neighbors and fuse into the identity with amplitude $C_{0\beta}$.

fective lattice $\tilde{\mathcal{L}}$ by means of an inhomogeneous coarse graining. Let

$$H = h^\diamond(0) + \sum_{r=0}^{\infty} h(r, r+1) \quad (8)$$

be the Hamiltonian on \mathcal{L} , where h^\diamond is a boundary term and $h(r, r+1) \equiv h$ is a (constant) two-site interaction term. The assumption that H is a fixed-point Hamiltonian implies that h is a (*two-site*)⁶ scaling operator with scaling dimension $\Delta = 2$. Let

$$K^{[t, t+1]} \equiv \sum_{r=r_t}^{r_{t+1}-1} h(r, r+1), \quad r_t \equiv (3^t - 1)/2 \quad (9)$$

be an operator that collects the 3^t two-site terms h included in the interval of sites $[r_t, r_{t+1}]$ of \mathcal{L} . Then the effective lattice $\tilde{\mathcal{L}}$ with sites labeled by $t \in \{0, 1, 2, \dots, \infty\}$, results from coarse graining \mathcal{L} in such a way that site $t \in \tilde{\mathcal{L}}$ corresponds to $O(3^t)$ sites of \mathcal{L} , see Fig. 3(i). Under the inhomogeneous coarse graining, the original Hamiltonian becomes

$$\tilde{H} = \tilde{h}^\diamond(0, 1) + \sum_{t=1}^{\infty} \Lambda^{1-t} \tilde{h}(t, t+1), \quad (10)$$

where $\tilde{h}^\diamond(0, 1)$ corresponds to $h^\diamond(0) + h(0, 1)$ in Eq. (8), Λ is just the scaling factor ($\Lambda = 3$) and the two-site term $\Lambda^{1-t} \tilde{h}(t, t+1)$ results from coarse graining $K^{[t, t+1]}$. For instance, $\tilde{h}(1, 2)$ comes from coarse graining $K^{[1, 2]} \equiv h(1, 2) + h(2, 3) + h(3, 4)$ as in Fig. 3(ii); the term $3^{-1} \tilde{h}(2, 3)$ comes from coarse graining $K^{[2, 3]}$ into $3^{-1} K^{[1, 2]}$, Fig. 3(iii), and then $K^{[1, 2]}$ into \tilde{h} as before; more generally, $K^{[t, t+1]}$ is first coarse grained into $3^{1-t} K^{[1, 2]}$ and then $K^{[1, 2]}$ again into \tilde{h} . To under-

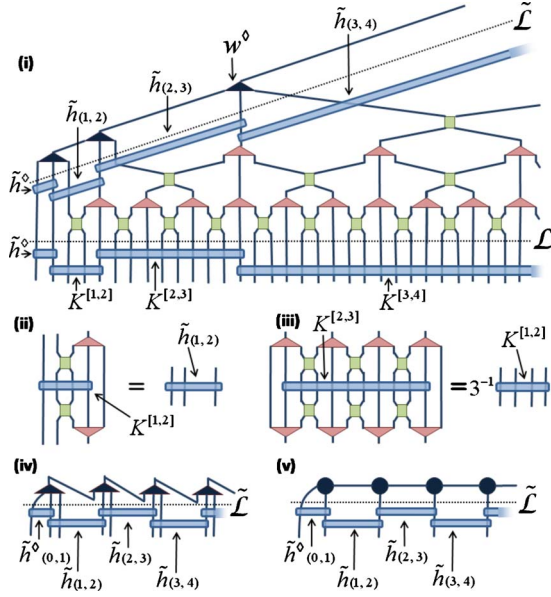


FIG. 3. (Color online) (i) The effective lattice $\tilde{\mathcal{L}}$ is obtained by coarse graining \mathcal{L} in an inhomogeneous way. Hamiltonian term $K^{[t,t+1]}$ involving 3^t sites in \mathcal{L} becomes the term $3^{1-t}\tilde{h}(t,t+1)$ on $\tilde{\mathcal{L}}$. (ii) Definition of $\tilde{h}^{[1,2]}$ in terms of $K^{[1,2]}$, u , and w . (iii) Applying one layer of coarse graining to $K^{[2,3]}$ produces $3^{-1}K^{[1,2]}$. (iv) Copies of w° are used to describe the ground state of \tilde{H} , Eq. (10). (v) The boundary of the MERA can be regarded as a homogeneous MPS on $\tilde{\mathcal{L}}$.

stand the origin of the scaling factor 3^{-t} , we notice that under coarse graining in the bulk, $K^{[t,t+1]}$ (made of 3^t terms h) becomes proportional to $K^{[t-1,t]}$ (made of 3^{t-1} terms h),

$$K^{[t,t+1]} \xrightarrow{\text{RG}} 3^{-1}K^{[t-1,t]}, \quad (t > 1), \quad (11)$$

where the factor $3^{-1} = 3^{-2} \times 3$ is due to the scaling dimension $\Delta=2$ of h (factor $3^{-\Delta} = 3^{-2}$) and the fact that each term h in $K^{[t-1,t]}$ comes from three terms h in $K^{[t,t+1]}$ (factor 3). Then, after $t-1$ iterations of the RG transformation, $K^{[t,t+1]}$ indeed becomes

$$K^{[t,t+1]} \xrightarrow{\text{RG}} 3^{1-t}K^{[1,2]}, \quad (t \geq 1). \quad (12)$$

The Hamiltonian \tilde{H} in Eq. (10) describes a semi-infinite chain of sites that interact with nearest neighbors with the same interaction term \tilde{h} , which is multiplied by a factor Λ^{1-t} decreasing exponentially fast with the distance to the boundary. Importantly, in spite of the boundary at $t=0$, the ground state of \tilde{H} can be well approximated with a homogeneous MPS, obtained by connecting together copies of the boundary isometry w° , Figs. 3(iii–iv). Moreover, the boundary scaling dimensions Δ_α° , which characterize polynomial decays of correlations in \mathcal{L} , describe exponential decays of correlations in $\tilde{\mathcal{L}}$,

$$\langle \phi_\alpha^\circ(t) \phi_\alpha^\circ(t') \rangle \approx e^{-\Delta_\alpha^\circ |t-t'|}, \quad (13)$$

thus extending the interpretation of the MERA as a lattice realization of the holographic principle, as reported in Ref. 13.

The effective Hamiltonian \tilde{H} is of the form derived by Wilson as part of his resolution of the Kondo problem.⁸ Notice, however, that while Wilson’s derivation was for free fermions and the limit $\Lambda \rightarrow 1$ was eventually taken, here we started with a generic critical Hamiltonian and Λ remains fixed at $\Lambda=3$. In a recent paper,¹⁴ Okunishi proposed an interesting generalization of Wilson’s NRG approach that also considered a generic critical Hamiltonian, although the scale $\Lambda > 1$ in Eq. (10) was simply introduced “by hand” as a regulator of the gapless spectrum and made very close to 1 (e.g., $\Lambda=1.02$) to avoid an “undesired perturbation” in its degeneracy structure and \tilde{h} was chosen to be simply equal to h .

Examples. To demonstrate the validity of the boundary MERA as an ansatz for boundary critical ground states, we analyze the critical quantum Ising and quantum XX models on a semi-infinite chain,

$$H_{\text{Ising}} = \eta X(0) - \sum_{r=0}^{\infty} [X(r)X(r+1) + Z(r+1)],$$

$$H_{\text{XX}} = \eta X(0) + \sum_{r=0}^{\infty} [X(r)X(r+1) + Y(r)Y(r+1)],$$

(14)

where X , Y , and Z are the Pauli matrices and the constant η determines whether the system has free BC ($\eta=0$) or fixed BC ($\eta=\pm 1$). For each model, bulk tensors u and w are first computed using the energy minimization algorithm for the scale invariant MERA discussed in Refs. 6 and 15. Then, for each choice of η , H is coarse grained into the effective Hamiltonian \tilde{H} of Eq. (10) and the boundary isometry w° is obtained with a simplified version (replacing the MERA with an MPS) of the same energy minimization algorithm.¹⁶ Figure 4 displays the expectation value $\langle Z(r) \rangle$ for the Ising model with both free and fixed BC and shows that the boundary MERA faithfully reproduces the scaling of observables in the presence of a boundary, in spite of the fact that the ansatz uses, arbitrarily close to the boundary, bulk tensors u and w that have been optimized in the absence of a boundary. Figure 5 shows some boundary scaling dimensions Δ_α° obtained by diagonalizing the boundary scaling superoperator \mathcal{S}° , Eq. (5). They appear organized according to the conformal towers of primary fields, as predicted by BCFT.¹¹ These scaling dimensions are remarkably accurate; for the Ising model the smallest scaling dimensions ($\Delta_\alpha^\circ \leq 3$) are reproduced with less than 0.2% error while for the quantum XX model ($\Delta_\alpha^\circ \leq 2.5$) the error is less than 0.4%.

In summary, we have proposed and demonstrated the use of entanglement renormalization techniques to study boundary critical phenomena. The boundary MERA, encoded in just three tensors (u, w, w°), naturally reproduces the expectation value of bulk scaling operators in the presence of a boundary, Eq. (7), while also yielding accurate boundary

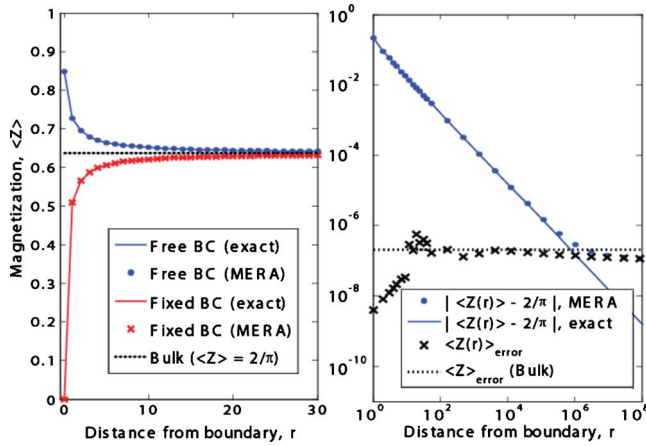


FIG. 4. (Color online) Left: expectation value $\langle Z(r) \rangle$ for the critical Ising model with free and fixed BC obtained with a boundary MERA. The exact solution approaches the bulk value $2/\pi$ as r^{-1} , i.e., $\Delta=1$. Right: error in $\langle Z(r) \rangle$ for free BC (similar to that for fixed BC). The nonvanishing expectation value of bulk scaling operators, Eq. (7), is accurately reproduced even thousands of sites away from the boundary.

scaling dimensions, Eq. (5). Moreover, the success of this ansatz, which accepts a holographic interpretation,¹³ unveils a surprisingly simple relation between the structure of ground-state wave function of critical spin chains with and without a boundary since the same bulk tensors (u, w) are used in both cases.

The present construction, based only on scale invariance, can be readily generalized to study two-dimensional lattice

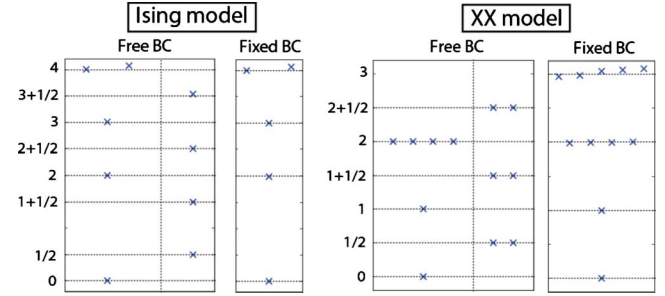


FIG. 5. (Color online) A few boundary scaling dimensions, organized in conformal towers (Ref. 11), for the quantum Ising and quantum XX models with free and fixed BC. The boundary MERA accurately reproduces the smallest scaling dimensions of each conformal tower.

systems with open boundaries, as well as to study systems with local defects and interfaces between different critical systems. By considering a different boundary isometry at each level of coarse graining, it is also possible to study boundary RG flows (e.g., from free BC to fixed BC). Finally, our results provide a numerical route to boundary conformal-field theory¹² that may find applications in areas ranging from condensed-matter physics (boundary critical behaviors and quantum impurity problems) to string theory (open strings and D-branes).

Support from the Australian Research Council (APA, Grants No. FF0668731 and No. DP0878830) and the Spanish Ministerio de Ciencia e Innovación (Grant No. RYC-2009-04318) is acknowledged.

¹G. Vidal, *Phys. Rev. Lett.* **99**, 220405 (2007).

²G. Vidal, *Phys. Rev. Lett.* **101**, 110501 (2008).

³M. Aguado and G. Vidal, *Phys. Rev. Lett.* **100**, 070404 (2008); R. König, B. W. Reichardt, and G. Vidal, *Phys. Rev. B* **79**, 195123 (2009).

⁴G. Evenbly and G. Vidal, *Phys. Rev. B* **81**, 235102 (2010); *New J. Phys.* **12**, 025007 (2010).

⁵V. Giovannetti, S. Montangero, and R. Fazio, *Phys. Rev. Lett.* **101**, 180503 (2008).

⁶R. N. C. Pfeifer, G. Evenbly, and G. Vidal, *Phys. Rev. A* **79**, 040301(R) (2009).

⁷S. Montangero, M. Rizzi, V. Giovannetti, and R. Fazio, *Phys. Rev. B* **80**, 113103 (2009); V. Giovannetti, S. Montangero, M. Rizzi, and R. Fazio, *Phys. Rev. A* **79**, 052314 (2009).

⁸K. G. Wilson, *Rev. Mod. Phys.* **47**, 773 (1975).

⁹S. R. White, *Phys. Rev. Lett.* **69**, 2863 (1992).

¹⁰M. Fannes, B. Nachtergaele, and R. F. Werner, *Commun. Math. Phys.* **144**, 443 (1992); S. Östlund and S. Rommer, *Phys. Rev. Lett.* **75**, 3537 (1995).

¹¹P. Di Francesco, P. Mathieu, and D. Senechal, *Conformal Field Theory* (Springer, New York, 1997).

¹²J. L. Cardy, *Nucl. Phys. B* **275**, 200 (1986); J. Cardy, in *Encyclopedia of Mathematical Physics*, edited by J.-P. Francoise, G. L. Naber, and T. S. Tsun (Elsevier, New York, 2006), pp. 333–340.

¹³B. Swingle, [arXiv:0905.1317](https://arxiv.org/abs/0905.1317) (unpublished).

¹⁴K. Okunishi, *J. Phys. Soc. Jpn.* **76**, 063001 (2007).

¹⁵G. Evenbly and G. Vidal, *Phys. Rev. B* **79**, 144108 (2009).

¹⁶We used $\chi=16$ for the boundary bond dimension, $\chi=28(54)$ for the bulk bond dimension of the quantum Ising (XX) model, and two transitional layers of tensors to mitigate the effect of irrelevant terms in Eq. (14) (Refs. 6 and 15).